Can we compute fMRI brain activation directly from k-space?

Daniel B. Rowe[1,2,*]
Department of Biophysics[1] and Division of Biostatistics[2]

Division of Biostatistics
Medical College of Wisconsin

Technical Report 54

September 2006

Division of Biostatistics
Medical College of Wisconsin
8701 Watertown Plank Road
Milwaukee, WI 53226
Phone:(414) 456-8280

Can we compute fMRI brain activation directly from k-space?

Daniel B. Rowe[1,2*]

[1]Department of Biophysics, [2]Division of Bistatistics,

Medical College of Wisconsin, Milwaukee, WI USA

KEY WORDS: image reconstruction, k-space, fMRI, complex data, Rowe-Logan

Abstract

In functional magnetic resonance imaging (fMRI), a process of determining statistically significant brain activation is commonly performed in terms of voxel time course measurements after image reconstruction. The image reconstruction and statistical activation processes are treated separately. In this manuscript, the relationship between complex-valued (Fourier) encoded k-space measurements and complex-valued image measurements from (Fourier) reconstructed images is described. The voxel time-series measurements are written in terms of spatio-temporal k-space measurements utilizing this spatial frequency k-space and image relationship. Voxel fMRI activation can be determined in image space for example using the Rowe-Logan complex-valued activation model [Rowe, D.B., and Logan, B.R. (2004). A complex way to compute fMRI activation. NeuroImage, 23 (3):1078-1092] in terms of the original k-space measurements. Additionally, the spatio-temporal covariance between reconstructed complex-valued voxel time series can be written in terms of the spatio-temporal covariance between complex-valued k-space measurements. Knowledge of the relationship between the spatio-temporal k-space measurements can be modeled in the more naturally acquired state rather than in a transformed state. This allows for the partitioning of the covariance matrix between the k-space measurements and hence voxel measurements into sources of covariation. Statistical associations between individual voxels or regions of interest can be quantified utilizing unmodeled sources of covariation.

1 Introduction

In functional magnetic resonance imaging (fMRI), the processes of image reconstruction (Kumar, et al., 1975; Haacke et al., 1999) and statistical activation (Bandettini et al., 1993; Friston et al., 1994) have been treated separately. The determination of statistically significant brain activation is in terms of voxel measurements after reconstruction. The relationship between the original k-space measurements and voxel measurements for each image is described. A permutation matrix is utilized to reorder the voxel measurements and statistical functional brain activation can be determined with complex-valued activation models (Nan and Nowak, 1999; Rowe and

*Corresponding Author: Daniel B. Rowe, Department of Biophysics, Medical College of Wisconsin, 8701 Watertown Plank Road, Milwaukee, WI 53226, dbrowe@mcw.edu.

Logan, 2004,2005; Rowe, 2005a,b). A map of these activation statistics can then thresholded to determine statistically significant activation while adjusting for multiple compariations (Logan and Rowe, 2004).

2 Methods

In fMRI, data generally consist of two-dimensional slices acquired from an echo-planar imaging (EPI) pulse sequence. The $p_y \times p_x$ dimensional complex-valued spatial frequency measurement S_C of a slice consists of a $p_y \times p_x$ dimensional matrix of true underlying noiseless complex-valued spatial frequencies S_{0C} and a $p_y \times p_x$ dimensional matrix of complex-valued measurement error E_C that can be represented as

$$S_C \quad = \quad (S_{0R} + iS_{0I}) \quad + \quad (E_R + iE_I) \tag{2.1}$$

where i is the imaginary unit while S_{0R}, S_{0I}, E_R and E_I are real and imaginary matrix valued parts of the true spatial frequencies and measurement noise. Let Ω_{Cx} and Ω_{Cy} be $p_x \times p_x$ and $p_y \times p_y$ complex-valued Fourier matrices such that

$$\Omega_{Cy} \quad = \quad \Omega_{Ry} \quad + \quad i \quad \Omega_{Iy} \quad \text{and} \quad \Omega_{Cx} \quad = \quad \Omega_{Rx} \quad + \quad i \quad \Omega_{Ix} \tag{2.2}$$

where Ω_{Ry} and Ω_{Rx} are real while Ω_{Iy} and Ω_{Ix} are imaginary matrix valued parts. Then, the $p_y \times p_x$ complex-valued inverse Fourier transformation reconstructed image R_C of S_C can be written as

$$\begin{array}{rcccccc} R_C & = & \Omega_{Cy} & * & S_C & * & \Omega_{Cx}^T \\ & = & \Omega_{Cy}(S_{0R} + iS_{0I})\Omega_{Cx}^T & & + & & \Omega_{Cy}(E_R + iE_I)\Omega_{Cx}^T \\ & = & R_{0C} & & + & & N_C \end{array}$$

where R_C has a true mean R_{0C} and measurement error N_C while "T" denotes transposition. If Ω_{Cx} is a Fourier matrix, it is $[\Omega_{Cx}]_{jk} = \kappa\left(\omega^{jk}\right)$ where $\kappa = 1$ and $\omega = \exp[-i2\pi(j-1)(k-1)/p_x]$ for the forward transformation while $\kappa = 1/p_x$ and $\omega = \exp[+i2\pi(j-1)(k-1)/p_x]$ for the inverse transformation, where $j, k = 1, ..., p_x$. The complex-valued matrices for reconstruction Ω_x and Ω_y need not be exactly Fourier matrices but may be Fourier matrices that include adjustments for magnetic field inhomogeneities derieved from phase maps or reconstruction matrices for other encoding procedures.

This inverse Fourier transformation image reconstruction process can be equivalently described as the pre-multiplication of the complex-valued spatial frequencies in the form of a real-valued vector s by a real-valued matrix representation Ω of the complex-valued Fourier matrices

$$\begin{array}{ccccc} r & = & \Omega & * & s \\ \begin{pmatrix} r_R \\ r_I \end{pmatrix} & = & \begin{pmatrix} \Omega_R & -\Omega_I \\ \Omega_I & \Omega_R \end{pmatrix} & * & \begin{pmatrix} s_R \\ s_I \end{pmatrix} \end{array} \tag{2.3}$$

where the real-valued representation r that is of dimension $2p_xp_y \times 1$ of the complex-valued image has a true mean and measurement error. The real-valued vector of spatial frequencies is formed by

$$s = \text{vec}(S_R^T, S_I^T)$$

where S_R and S_I denote the real and imaginary parts of S_C and vec$(\cdot)$ denotes the vectorization operator that stacks the columns of its matrix argument. In addition, the matrix elements of Ω are

$$\Omega_R = [(\Omega_{yR} \otimes \Omega_{xR}) - (\Omega_{yI} \otimes \Omega_{xI})] \quad (2.4)$$

$$\Omega_I = [(\Omega_{yR} \otimes \Omega_{xI}) + (\Omega_{yI} \otimes \Omega_{xR})] \quad (2.5)$$

where $\otimes$ denotes the Kronecker product that multiplies every element of its first matrix argument by its entire second matrix argument. If the mean and covariance of the spatial frequency measurement vector s that is of dimension $2p_xp_y \times 1$ are s_0 and Γ, then the mean and covariance of the reconstructed voxel measurements r are Ωs_0 and $\Omega\Gamma\Omega^T$.

In fMRI, a series of the previously described slices are acquired. Denote the $p_y \times p_x$ random complex-valued spatial frequency matrix at time t as $S_{Ct} = S_{0Ct} + E_{Ct}$ and define $s_t = \text{vec}(S_{Rt}^T, S_{It}^T)$, where S_{Rt} and S_{It} are the real and imaginary parts of S_{Ct} for time points $t = 1, ..., n$. Define the total number of voxels in the image, which is the same as the number of complex-valued k-space measurements to be $p = p_xp_y$. This sequence of measured spatial frequency vectors can be collected into a $2p \times n$ matrix $S = (s_1, ..., s_n)$ where the t^{th} column contains the p real k-space measurements stacked upon the p imaginary k-space measurements for time t. Having done this, n reconstructed images can be formed by the $2p \times n$ matrix $R = \Omega S$ where the t^{th} column of R contains the p real voxel measurements stacked upon the p imaginary voxel measurements for time t, $t = 1, ..., n$.

The k-space measurements and the image voxel measurements can be stacked as $s = \text{vec}(S)$ and $r = \text{vec}(R)$. Note that s and r and have been redefined from their previous definition. If the mean and covariance of the $2np \times 1$ vector of spatial frequency measurements s are s_0 and Δ, then the mean and covariance of the $2np \times 1$ vector of reconstructed voxel measurements r are $(I_n \otimes \Omega)s_0$ and $(I_n \otimes \Omega)\Delta(I_n \otimes \Omega^T)$. For example, if the k-space measurements were taken to be temporally independent, then $\Gamma = I_n \otimes \Gamma$ and $\text{cov}(r) = I_n \otimes (\Omega\Gamma\Omega^T)$. Thus, we have described the fMRI voxel measurements as a linear function of the fMRI k-space measurements. We can alternatively organize the voxel measurements by stacking the first set of p columns of R^T upon the second set of p columns of R^T to form a matrix Y. Having done this, the j^{th} column of the resulting data matrix Y of dimension $2n \times p$ contains the n real voxel measurements stacked upon the n imaginary voxel measurements for voxel j, $j = 1, ..., p$. The voxel measurements Y can be described with the complex fMRI model (Rowe and Logan, 2005) as

$$Y = \left[\begin{pmatrix} C_1X\beta_1 \\ S_1X\beta_1 \end{pmatrix}, ..., \begin{pmatrix} C_pX\beta_p \\ S_pX\beta_p \end{pmatrix} \right] + \left[\begin{pmatrix} \eta_{R1} \\ \eta_{I1} \end{pmatrix}, ..., \begin{pmatrix} \eta_{Rp} \\ \eta_{Ip} \end{pmatrix} \right] \quad (2.6)$$

where C_1 and S_1 are diagonal matrices with cosine and sine tems respectively. Different activation modeles are found by different choices of the C and S matrices. The complex constant phase model (Rowe and Logan, 2004) can be found with $C_j = I_n \cos\theta_j$ and $S_j = I_n \sin\theta_j$ where j indexes the j^{th} voxel. The unrestricted phase or magnitude only model can be found by by selecting the t^{th} element of C_j and S_j to be $C_{jt} = \cos\theta_{jt}$ and $S_{jt} = \sin\theta_{jt}$, where θ_{jt} is unique for each j and t. The complex model for both magnitude and phase (Rowe,

2005) can be found by choosing the phase $\theta_{jt} = u_t^T \gamma$ where u_t is the t^{th} row of a phase design matrix U and γ are phase regression coefficients.

This can be rearranged and written with $y = \text{vec}(Y)$ as

$$\begin{bmatrix} \begin{pmatrix} y_{R1} \\ y_{I1} \end{pmatrix} \\ \vdots \\ \begin{pmatrix} y_{Rp} \\ y_{Ip} \end{pmatrix} \end{bmatrix} = \begin{bmatrix} \begin{pmatrix} C_1X & 0 \\ 0 & S_1X \end{pmatrix} & & 0 \\ & \ddots & \\ 0 & & \begin{pmatrix} C_pX & 0 \\ 0 & S_pX \end{pmatrix} \end{bmatrix} \begin{bmatrix} \begin{pmatrix} \beta_1 \\ \beta_1 \end{pmatrix} \\ \vdots \\ \begin{pmatrix} \beta_p \\ \beta_p \end{pmatrix} \end{bmatrix} + \begin{bmatrix} \begin{pmatrix} \eta_{R1} \\ \eta_{I1} \end{pmatrix} \\ \vdots \\ \begin{pmatrix} \eta_{Rp} \\ \eta_{Ip} \end{pmatrix} \end{bmatrix} \tag{2.7}$$

where $y = (y_{R1}^T, y_{I1}^T, ..., y_{Rp}^T, y_{Ip}^T)^T$ is a vector containing the real and imaginary reconstructed voxel measurements and $\eta = (\eta_{R1}^T, \eta_{I1}^T, ..., \eta_{Rp}^T, \eta_{Ip}^T)^T$ is a vector containing the real and imaginary errors of the reconstructed voxel measurements. The model can simply be written as $y = \mu + \epsilon$. For example, with constant phase model, the mean is $\mu = (I_{2p} \otimes X)[(\cos\theta_1, \sin\theta_1) \otimes \beta_1^T, ..., (\cos\theta_p, \sin\theta_p) \otimes \beta_p^T]^T$.

The rearrangement of the voxel measurements from r to y is a linear transformation and can be achieved through a permutation matrix P (described in Appendix A) to form $y = Pr$. In terms of the original k-space measurements the voxel time courses are $y = P(I_n \otimes \Omega)\text{vec}(\text{vec}(S_{R1}^T, S_{I1}^T), ..., \text{vec}(S_{Rn}^T, S_{In}^T))$. A permutation matrix is a square matrix that can be obtained by permuting (rearranging) either the columns or rows of an identity matrix (Harville, 1999). A permutation matrix is of full rank and therefore nonsingular and also invertible. Having done this linear transformation, the mean and covariance of y are $\mu = P(I_n \otimes \Omega)s_0$ and $\Lambda = P(I_n \otimes \Omega)\Delta(I_n \otimes \Omega^T)P^T$. Since the matrices Ω and P that convert k-space measurements s to voxel measurements y are known *a priori*, the expression $y = P(I_n \otimes \Omega)s$ can be inverted to write $s = (I_n \otimes \Omega^{-1})P^{-1}y$ in terms of the parameters as

$$\begin{pmatrix} s_1 \\ \vdots \\ s_n \end{pmatrix} = \underbrace{P^{-1}\left[I_n \otimes \Omega^{-1}(I_2 \otimes X)\right]}_{\text{Known}} \begin{pmatrix} \beta_1 \cos\theta_1 \\ \beta_1 \sin\theta_1 \\ \vdots \\ \beta_p \cos\theta_p \\ \beta_p \sin\theta_p \end{pmatrix} + \begin{pmatrix} \epsilon_1 \\ \vdots \\ \epsilon_n \end{pmatrix} \tag{2.8}$$

then the optimization for the regression coefficients (β) and phases (θ) can be performed in k-spacesto yield the same parameter estimates. Activations can then be computed from Rowe's complex activation models.

Using ordinary least squares or a normal distributional specification on the errors, the voxel-wise regression coefficients and phases can be determined to yield the same point estimators as in Logan and Rowe (2004). The Rowe-Logan unconstrained alternative hypothesis estimators (with hats) for H_1: $C\beta \neq 0$ along with the constrained null hypothesis estimators (with tildes) for H_0: $C\beta = 0$ in voxel j are

$$\begin{array}{lllllll} \hat{\theta}_j & = & \frac{1}{2}\tan^{-1}\left[\frac{\hat{\beta}_{Rj}^T(X'X)\hat{\beta}_{Ij}}{(\hat{\beta}_{Rj}^T(X'X)\hat{\beta}_{Rj} - \hat{\beta}_{Ij}^T(X'X)\hat{\beta}_{Ij})/2}\right] & \tilde{\theta}_j & = & \frac{1}{2}\tan^{-1}\left[\frac{\hat{\beta}_{Rj}^T\Psi(X'X)\hat{\beta}_{Ij}}{(\hat{\beta}_{Rj}^T\Psi(X'X)\hat{\beta}_{Rj} - \hat{\beta}_{Ij}^T\Psi(X'X)\hat{\beta}_{Ij})/2}\right] \\ \hat{\beta}_j & = & \hat{\beta}_{Rj}\cos\hat{\theta}_j + \hat{\beta}_{Ij}\sin\hat{\theta}_j & \tilde{\beta}_j & = & \Psi\left[\hat{\beta}_{Rj}\cos\tilde{\theta}_j + \hat{\beta}_{Ij}\sin\tilde{\theta}_j\right] \end{array} \tag{2.9}$$

where C is an $r \times (q+1)$ matrix of full row rank, $\Psi = I_{q+1} - (X'X)^{-1}C'[C(X'X)^{-1}C']^{-1}C$, $\hat{\beta}_{Rj} = (X'X)^{-1}X'y_{Rj}$, and $\hat{\beta}_{Ij} = (X'X)^{-1}X'y_{Ij}$, while y_{Rj} and y_{Ij} are the $n \times 1$ vectors of real and imaginary voxel observations.

The variances and covariances for example with a specification of uncorrelated temporal k-space measurement vectors (s_t) yields the covaraince matrix $\Lambda = I_n \otimes \Omega\Gamma\Omega^T$ for the voxel measurements. Define the voxel measurement covariance matrix to be $\Sigma = \Omega\Gamma\Omega^T$. Having estimated the voxel-wise regression coefficients and phases, we can estimate the mean of the vector of voxel measurements y by $\hat{\mu}$ (under the alternative hypothesis) and the mean of the matrix of voxel measurements R by $\hat{M} = \overline{\text{vec}}(P^{-1}\hat{\mu})$. Here $\overline{\text{vec}}(\cdot)$ is the operator that is the inverse operation of the vec$(\cdot)$ operator. The voxel covariance matrix is

$$\Sigma = \begin{bmatrix} \Sigma_{11} & \Sigma_{12} \\ \Sigma_{12}^T & \Sigma_{22} \end{bmatrix} \tag{2.10}$$

where the partitioned matrix elements are

$$\begin{aligned}
\Sigma_{11} &= \Omega_R\Gamma_{11}\Omega_R^T - \Omega_I\Gamma_{12}^T\Omega_R^T - \Omega_R\Gamma_{12}\Omega_I^T + \Omega_I\Gamma_{22}\Omega_I^T && (2.11)\\
\Sigma_{12} &= \Omega_R\Gamma_{11}\Omega_I^T - \Omega_I\Gamma_{12}^T\Omega_I^T + \Omega_R\Gamma_{12}\Omega_R^T - \Omega_I\Gamma_{22}\Omega_R^T && (2.12)\\
\Sigma_{22} &= \Omega_I\Gamma_{11}\Omega_I^T + \Omega_R\Gamma_{12}^T\Omega_I^T + \Omega_I\Gamma_{12}\Omega_R^T + \Omega_R\Gamma_{22}\Omega_R^T\ . && (2.13)
\end{aligned}$$

and Γ has been partitioned similar to Σ. The voxel covariance matrix Σ can now be estimated by $\hat{\Sigma} = (R - \hat{M})(R - \hat{M})^T/n$ where

With the physically motivated specification of the same k-space covariance Γ_W within the real-imaginary channels and k-space covariance between the real-imaginary channels Γ_B with the previous uncorrelated temporal k-space measurements, the voxel covaraince matrix becomes

$$\Sigma = \begin{bmatrix} \Sigma_W & \Sigma_B \\ \Sigma_B^T & \Sigma_W \end{bmatrix} \tag{2.14}$$

where the equal within real and within imaginary channel covariances result from a skew-symmetric k-space covariance specification ($\Gamma_B^T = -\Gamma_B$) corresponding to a complex normal distribution and

$$\begin{aligned}
\Sigma_W &= \Omega_R\Gamma_W\Omega_R^T - \Omega_I\Gamma_B^T\Omega_R^T - \Omega_R\Gamma_B\Omega_I^T + \Omega_I\Gamma_W\Omega_I^T && (2.15)\\
\Sigma_B &= \Omega_R\Gamma_W\Omega_I^T - \Omega_I\Gamma_B^T\Omega_I^T - \Omega_R\Gamma_B\Omega_R^T - \Omega_I\Gamma_W\Omega_R^T\ . && (2.16)
\end{aligned}$$

We can estimate the covariance matrices under the alternative hypothesis by

$$\begin{aligned}
\hat{\Sigma}_W &= [(R_R - \hat{M}_R)(R_R - \hat{M}_R)^T + (R_I - \hat{M}_I)(R_I - \hat{M}_I)^T]/(2n) && (2.17)\\
\hat{\Sigma}_B &= [(R_R - \hat{M}_R)(R_I - \hat{M}_I)^T + (R_I - \hat{M}_I)(R_R - \hat{M}_R)^T]/(2n)\ . && (2.18)
\end{aligned}$$

and under the null hypothesis similarly find

$$\begin{aligned}
\tilde{\Sigma}_W &= [(R_R - \tilde{M}_R)(R_R - \tilde{M}_R)^T + (R_I - \tilde{M}_I)(R_I - \tilde{M}_I)^T]/(2n) && (2.19)\\
\tilde{\Sigma}_B &= [(R_R - \tilde{M}_R)(R_I - \tilde{M}_I)^T + (R_I - \tilde{M}_I)(R_R - \tilde{M}_R)^T]/(2n)\ . && (2.20)
\end{aligned}$$

It should be noted that the j^{th} diagonal elements of $\hat{\Sigma}_W$ and $\tilde{\Sigma}_W$ are equivalent to those given in Rowe and Logan (2004)

$$\hat{\sigma}_j^2 = \frac{1}{2n} \begin{bmatrix} y_{Rj} - X\hat{\beta}_j \cos\hat{\theta}_j \\ y_{Ij} - X\hat{\beta}_j \sin\hat{\theta}_j \end{bmatrix}^T \begin{bmatrix} y_{Rj} - X\hat{\beta}_j \cos\hat{\theta}_j \\ y_{Ij} - X\hat{\beta}_j \sin\hat{\theta}_j \end{bmatrix} \tag{2.21}$$

$$\tilde{\sigma}_j^2 = \frac{1}{2n} \begin{bmatrix} y_{Rj} - X\tilde{\beta}_j \cos\tilde{\theta}_j \\ y_{Ij} - X\tilde{\beta}_j \sin\tilde{\theta}_j \end{bmatrix}^T \begin{bmatrix} y_{Rj} - X\tilde{\beta}_j \cos\tilde{\theta}_j \\ y_{Ij} - X\tilde{\beta}_j \sin\tilde{\theta}_j \end{bmatrix} . \tag{2.22}$$

Additionally, voxel-wise activations will be the same as in Rowe and Logan (2004). Then the generalized likelihood ratio statistic for the complex fMRI activation model is

$$-2\log\lambda_j = 2n\log\left(\tilde{\sigma}_j^2/\hat{\sigma}_j^2\right) . \tag{2.23}$$

This statistic has a large sample χ_r^2 distribution. Note that when $r = 1$, two-sided testing can be done using the signed likelihood ratio test given by

$$z_j = \text{Sign}(C\hat{\beta}_j)\sqrt{-2\log\lambda_j}, \tag{2.24}$$

which has a large sample standard normal distribution under the null hypothesis. Alternatively with $r = 1$, a Wald type statistic can be formed

$$w_j = C\hat{\beta}_j/\sqrt{\hat{\sigma}_j^2 C(X^TX)^{-1}C'}, \tag{2.25}$$

which also has a large sample standard normal distribution under the null hypothesis. A map of these activation statistics is then thresholded while adjusting for multiple compariations (Logan and Rowe, 2004). However, correlations between voxels are characterized in terms of spatio-temporal correlations between k-space measurements.

The spatio-temporal covariances between the complex-valued voxel measurements Λ can now be described in terms of the spatio-temporal covariances between the complex-valued k-space measurements Δ. The covariance of the complex-valued k-space measurements may be due to independent sources such as spatio-temporal independent noise Δ_I, correlated nonphysiologic noise Δ_N such as measurement autocorrelation along the EPI trajectory or correlation induced by k-space corrections, and true physiologic processes Δ_P so that $\Delta = \Delta_P + \Delta_N + \Delta_I$. One could apply temporal filtering or pre-whitening to the k-space measurements. The voxel covariance and hence correlation can also be decomposed into the corresponding covariance components, $\Lambda = \Lambda_P + \Lambda_N + \Lambda_I$. Statements about voxel associations due to physiological processes could be made using only $\Lambda_P = P(I_n \otimes \Omega)\Delta_P(I_n \otimes \Omega^T)P^T$.

After fitting the fMRI model to the voxel image time courses, we can transform the residual images into spatial frequencies (k-space) and estimate the correlation due to non-physiologic sources Δ_N. The spatial frequances can then be temporally pre-whitened, transformed back into residual images then the noise variation Σ_W re-estimated.

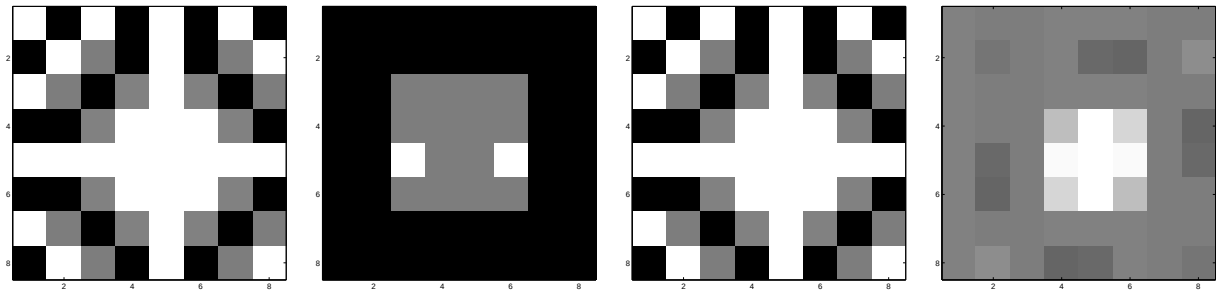

(a) Forward matrix $\bar{\Omega}_{yR}$ (c) Image real R_R (e) Forward matrix $\bar{\Omega}_{xR}$ (g) Spatial frequencies S_R

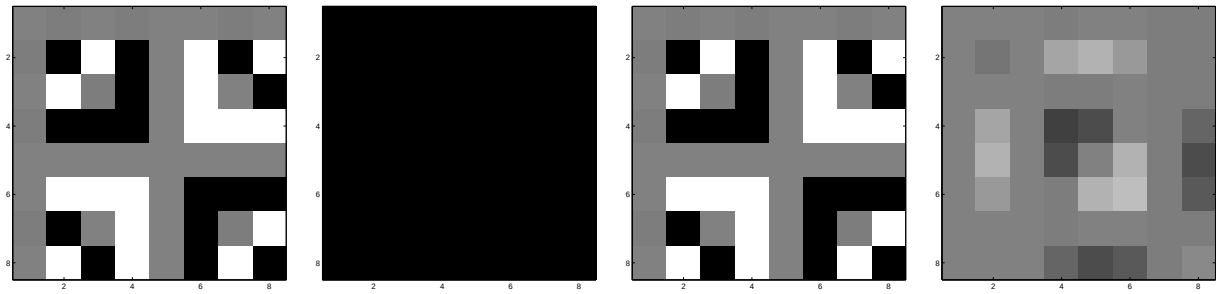

(b) Forward matrix $\bar{\Omega}_{yI}$ (d) Image imaginary R_I (f) Forward matrix $\bar{\Omega}_{xI}$ (h) Spatial frequencies S_I

Figure 1: Complex-valued 2D forward Fourier transform

3 Example

In order to demonstrate the previously described methodology a simulated example is presented. An 8×8 image R_C as displayed in Figure 1 with real part R_R given in Figure 1c and imaginary part R_I in Figure 1d is utilized to mimic a magnetic resonance echo planar imaging experiment. The spatial frequency (k-space) values S_C associated with this complex-valued image can be found by pre-multiplying the complex-valued image R_C with real image part R_R in Figure 1c and imaginary image part R_I in Figure 1d by the complex-valued forward Fourier matrix $\bar{\Omega}_{Cy}$ presented as an image with real part $\bar{\Omega}_{Ry}$ in Figure 1a and imaginary part $\bar{\Omega}_{Iy}$ in Figure 1b then post-multiplying the result by the transpose of the symmetric forward Fourier matrix $\bar{\Omega}_{Cx}$ presented as an image with real part $\bar{\Omega}_{Rx}$ in Figure 1e and imaginary part $\bar{\Omega}_{Ix}$ in Figure 1f. The spatial frequency (k-space) values S_C for the complex-valued image with real image part R_R in Figure 1c and imaginary image part R_I in Figure 1d are presented as an image with real part S_R given in Figure 1g and imaginary part S_I in Figure 1h. Note that the image does not have to be square.

The complex-valued image R_C with real image part R_R in Figure 1c and imaginary image part R_I in Figure 1d can be recovered as seen in Figure 2. The process of recovering the original complex-valued image R_C is to pre-multiply the complex-valued spatial frequency (k-space) values S_C with real image part S_R in Figure 2c and

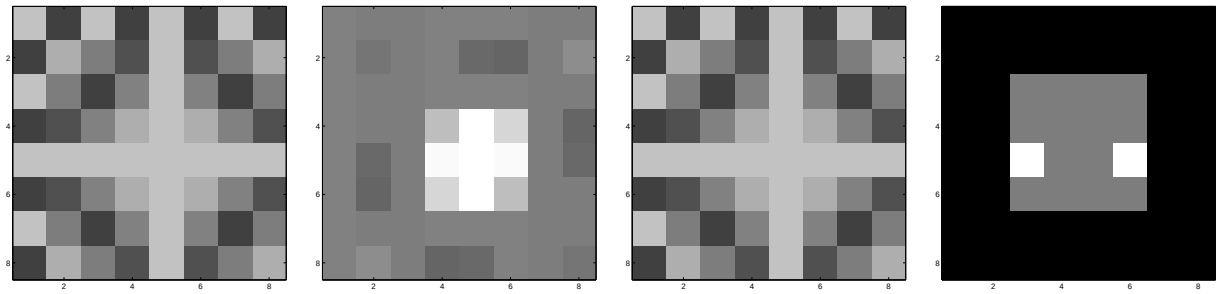

(a) Inverse matrix Ω_{yR} (c) Spatial frequencies S_R (e) Inverse matrix Ω_{xR} (g) Image real R_R

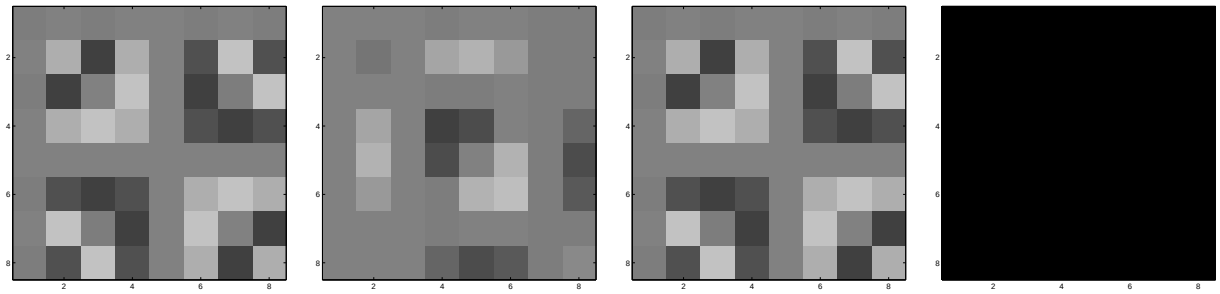

(b) Inverse matrix Ω_{yI} (d) Spatial frequencies S_I (f) Inverse matrix Ω_{xI} (h) Image imaginary R_I

Figure 2: Complex-valued 2D inverse Fourier transform

imaginary image part S_I in Figure 2d by the complex-valued inverse Fourier matrix Ω_{Cy} presented as an image with real part Ω_{Ry} in Figure 2a and imaginary part Ω_{Iy} in Figure 2b then post-multiply the result by the transpose of the symmetric inverse Fourier matrix Ω_{Cx} presented as an image with real part Ω_{Rx} in Figure 2e and imaginary part Ω_{Ix} in Figure 2f. The recovered complex-valued image R_C is presented with real part R_R in Figure 2g and imaginary part R_I in Figure 2h.

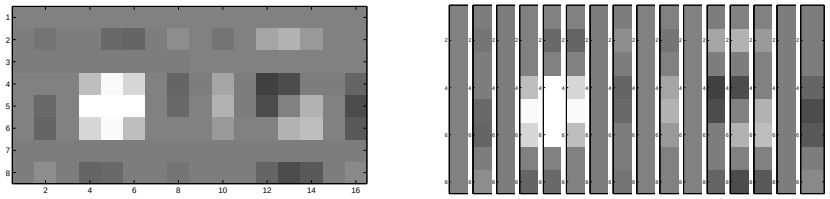

(a) Spatial frequencies $S^T = (S_R^T, S_I^T)$ (b) Partitioned spatial frequencies S^T

Figure 3: Matrix to vector spatial frequency (k-space) values.

The inverse Fourier transform fMRI reconstruction process can be equivalently described as follows with a

real-valued representation often called an isomorphism in mathematics. To use this representation, join the transpose of the real and imaginary parts of the spatial frequency (k-space) values given in Figure 2c and Figure 2d respectively that are of dimension $p_y \times p_x$ into a single real-valued matrix $S^T = (S_R^T, S_I^T)$ that is of dimension $p_x \times 2p_y$ as in Figure 3a. Then stack the columns of S^T as shown partitioned in Figure 3b into a single vector $s = \text{vec}(S_R^T, S_I^T)$ as presented in Figure 4b. This gives us a real-valued vector representation of the matrix of spatial frequency (k-space) values.

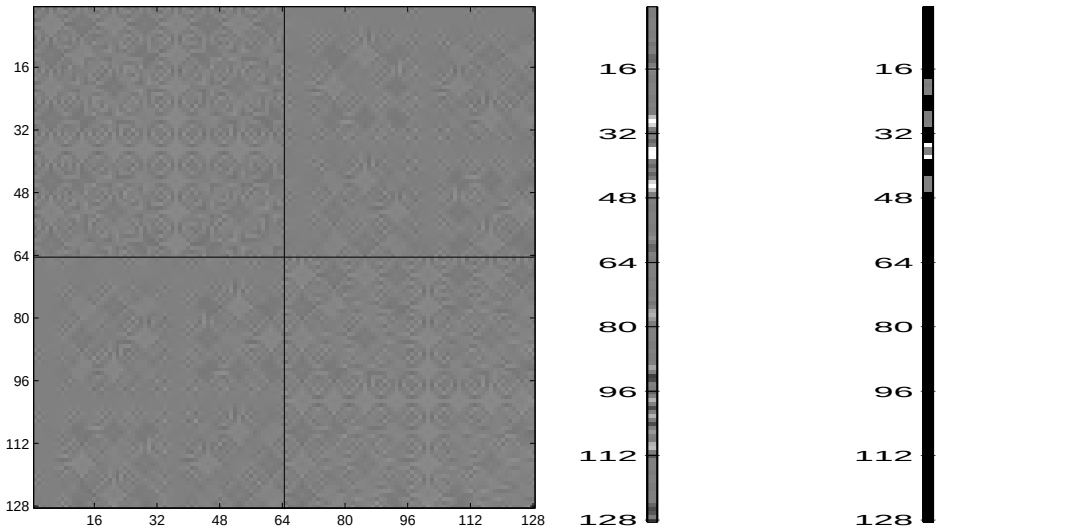

(a) reconstruction matrix Ω (b) frequency vector s (c) image vector r

Figure 4: Isomorphism for complex-valued 2D inverse Fourier Transform

The real-valued vector representation of the spatial frequency (k-space) values in Figure 4b is then pre-multiplied by the (inverse Fourier) reconstruction matrix Ω given in Figure 4a as described in Equation 2.3 to produce a vector representation of the image voxel measurements given in Figure 4c as described in Equation 2.3. The vector of voxel measurements is partitioned then arranged as in Figure 5a and formed into a single matrix image as in Figure 5b where the first (last) eight columns are the transpose of the real (imaginary) part of the image.

The previously described data for a single image is expanded upon to mimic an fMRI experiment. The complex-valued image in Figure 1c and Figure 1d is taken as the mean "active" or "on" image and a duplicate of it with the two white voxels replaced by grey voxels are used as the mean "inactive" or "off" images. For illustrative purposes, a single replicate of eight on images followed by eight off images that form a single block from an experiment with eight blocks is initially presented. Subsequently all eight blocks are examined. Eight column vectors of the spatial frequencies for the true mean "on" image are joined into a matrix with eight column vectors of the spatial frequencies for the true mean "off" image as in Figure 6b. Each column in Figure 6b is the

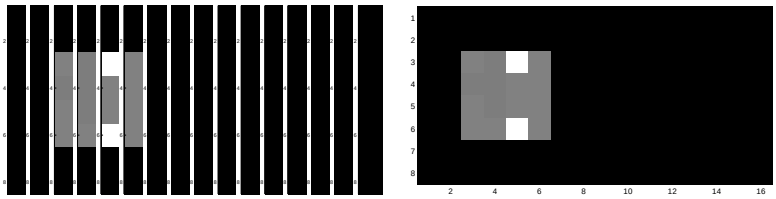

(a) partitioned images R^T

(b) combined image $R^T = (R_R^T, R_I^T)$

Figure 5: Vector to matrix image values.

vector form of the spatial frequencies for an image similar to that in Figure 4b.

The mean on images contained voxels with values $\beta_0 = 0$ and $\beta_1 = 0$ outside a four by four by four internal region, inactive gray voxels within the four by four region with values $\beta_0 = \text{SNR} * \sigma$ and $\beta_1 = 0$, along with two active voxels with value $\beta_0 = \text{SNR} * \sigma$ and $\beta_1 = \text{CNR} * \sigma$. Activation parameter values were SNR= 30, CNR= 1 and $\sigma = .05$. In this parameterization, SNR denotes the temporal signa-to-noise ratio, CNR denotes the functional contrast-to-noise ratio, and σ denotes the voxel standard deviation.

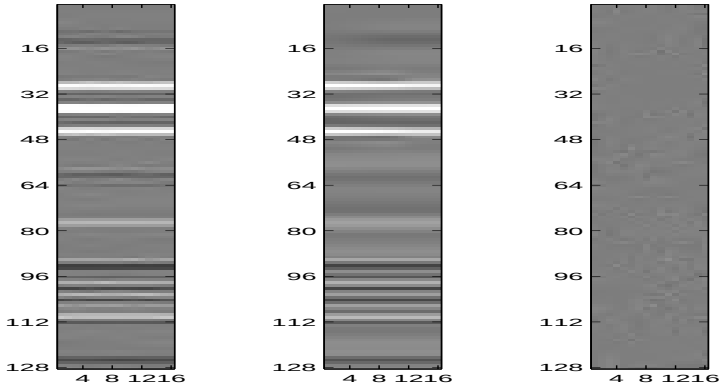

(a) noisy S

(b) true S_0

(c) error E

Figure 6: Noisy spatial frequency (k-space) values.

Independent noise column vectors ϵ_t as seen in Figure 6c are generated from a normal distribution with zero mean vector and covaiance matrix $\Gamma = \gamma^2\ \Gamma_1 \otimes \Gamma_2 \otimes \Gamma_3$. This covariance structure mimics temporal autocorrelation along the echo planar imaging (EPI) trajectory along with correlation between real and imaginary parts. The covariance matrix was formed with Γ_1, Γ_2, and Γ_3 taken to be unit variance correlation matrices while γ was taken to be $\gamma^2 = p_x p_y\ \sigma^2$. The $p_y \times p_y$ correlation matrix Γ_1 is taken to be an AR(1) correlation matrix with $(i,j)^{th}$ element $\varrho_1^{|i-j|}$ where $\varrho_1 = 0.25$, the 2×2 correlation matrix Γ_2 is taken to have an off diagonal correlation

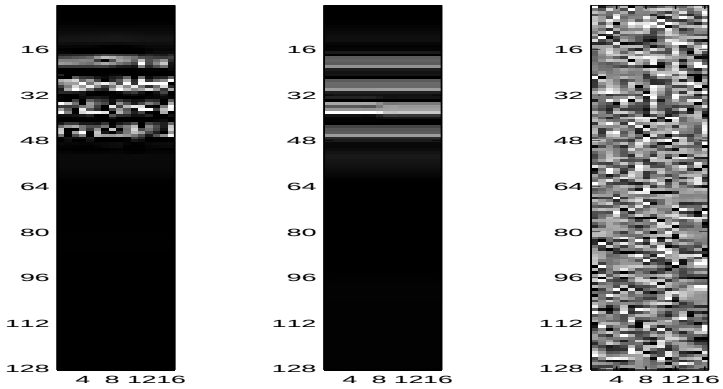

(a) noisy R=ΩS (b) true R_0=ΩS_0 (c) error N=ΩE

Figure 7: Reconstructed noisy images.

of $\varrho_2 = .5$ while the $p_x \times p_x$ correlation matrix Γ_3 is taken to be an AR(1) correlation matrix with $(i,j)^{th}$ element $\varrho_3^{|i-j|}$ where $\varrho_3 = 0.5$.

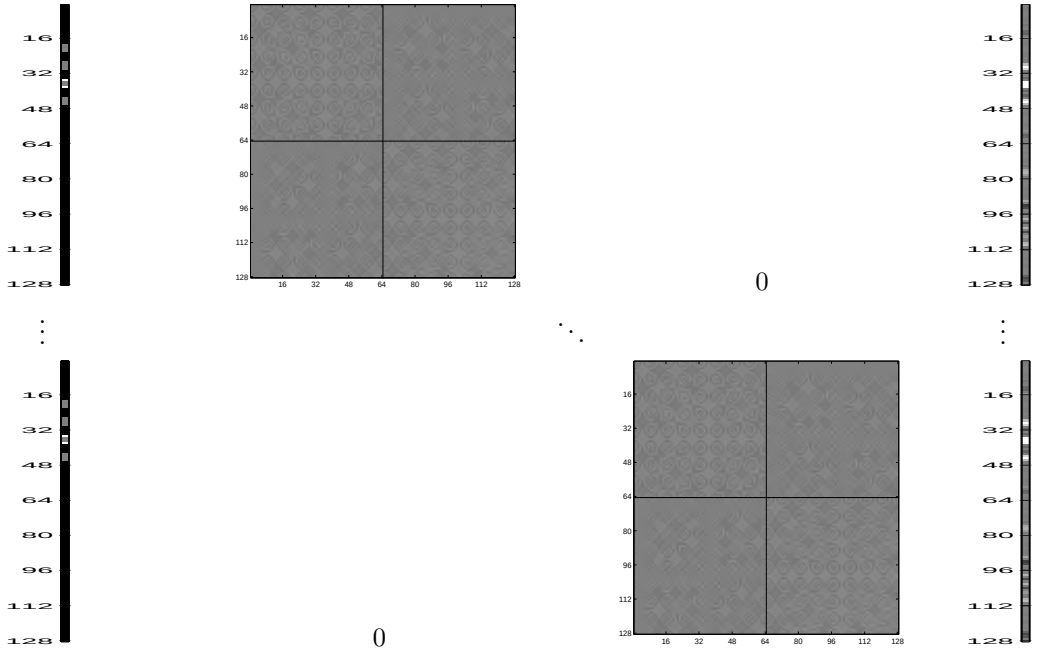

(a) noisy r (b) reconstruction matrix $(I_n \otimes \Omega)$ (c) noisy s

Figure 8: Reconstructed vectorized noisy images.

Each matrix image in Figure 6a, b, and c was pre-multiplied by the (inverse Fourier transform) image reconstruction matrix Ω given in Equation 2.3 and presented in Figure 4a. The results of this pre-multiplication

(a) voxel orderd y (b) permutation matrix P (c) image orderd r

Figure 9: Reordered reconstructed voxels.

can be seen in Figure 7a, b, and c. The columns of $R = \Omega S$ in Figure 7a are real and imaginary parts for each noisy image. The noisy image in Figure 7a the sum of the noiseless image in Figure 7b and the measurement noise presented as an image in Figure 7. However, we would like real and imaginary parts for each noisy voxel. As described in Section 2, we can vectorize R and S to yield $r = vec(R)$ and $s = vec(S)$ as seen in Figure 8. The vector s of noisy spatial frequency (k-space) values as presented in Figure 8c is pre-multiplied by a block diagonal matrix with Ω along the diagonal as displayed in Figure 8b to produce a vector of noisy image measurements r as shown in Figure 8a.

Now we can convert the vector r, displayed in Figure 8a that has values arranged that are reals and imaginaries stacked for images, to the vector y, that has values arranged that are reals and imaginaries stacked for voxels. We can convert from the vector r which is presented in Figure 9c to the vector y which is shown in Figure 9a via a permutation matrix P, a portion of which is displayed in Figure 9b. Now with the y vector being arranged as real and imaginary observations in each voxel as described in Equation 2.7, we can apply the complex activation models (Rowe and Logan, 2004). The regression coefficients β, the phase angle θ, and the variance σ^2 are estimated under both the null and alternative hypotheses as described in Eqution 2.9 then activation computed. In Figures 10a and c are the unthresholded activation maps for the magnitude-only and complex-valued activation methods respectively. In Figures 10b and d are the Bonferroni 5% thresholded activation maps for the magnitude-only and complex-valued activation techniques respectively.

As desccribed in Equation 2.10 of Section 3, we can also estimate covariance between voxels, $\hat{\Sigma}$. Again, note that the j^{th} diagonal element of $\hat{\Sigma}_W$ from Equation 2.17 is exactly $\hat{\sigma}_j^2$ from Rowe-Logan (2004) complex model. The sample voxel correlation from $\hat{\Sigma}_W$ described in Equation 2.17 is displayed in Figure 11a with theoretical value presented in Figure 11b. The sample correlation from $\hat{\Gamma} = \Omega^{-1}\hat{\Sigma}(\Omega^T)^{-1}$ is given in Figure 11c with theoretical

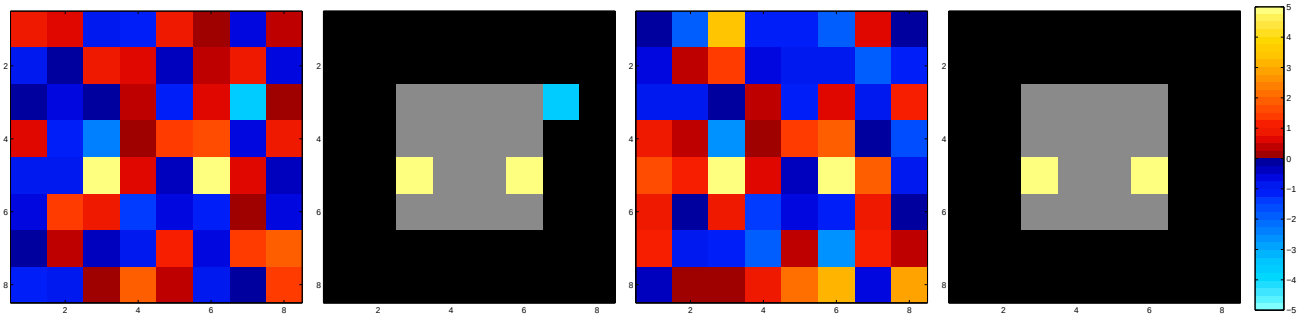

(a) Magnitude unthresholded (b) Magnitude thresholded (c) Complex unthresholded (d) Complex thresholded

Figure 10: Activation maps. Bonferroni 5% threshold.

value in Figure 11d. Note the similarity between the sample values and the theoretical values in Figures 11a and c to the theoretical values in Figures 11b and d even for the small sample size.

4 Discussion

Complex-valued voxel measurements have been written in terms of the original complex-valued k-space measurements. This allows the computation of statistically significant fMRI brain activation directly from the original k-space measurements but in image space. The correlation between voxel measurements can also be written in terms of correlation between k-space measurements. Since the covariance matrix between the k-space measurements and hence voxel measurements can be partitioned into individual sources of covariation, statistical associations between individual voxels or regions of interest could be quantified utilizing unmodeled sources of covariation.

Acknowledgments

This work was supported in part by NIH EB00215 and AG020279.

A Permutation Matrix

The elements of the permutation matrix P are all zero except for a single 1 in each row. The t^{th} row, $t = 1, ..., n$ within the first set of n rows of the permutation matrix P that form the n real measurements within the first voxel have a 1 in column $t = 0p + 1, 2p + 1, 4p + 1, ..., 2(n - 1)p + 1$. The t^{th} row within the second set of n rows of the permutation matrix P that form the n imaginary measurements within the first voxel have a 1 in column $t = p + 1, 3p + 1, 5p + 1, ..., 2(n - 1)p + p + 1$. The t^{th} row within the third set of n rows of the permutation matrix P that form the n real measurements within the second voxel have a 1 in column $t = 0p + 2, 2p + 2, 4p + 2, ..., 2(n - 1)p + 2$. The t^{th} row within the fourth set of n rows of the

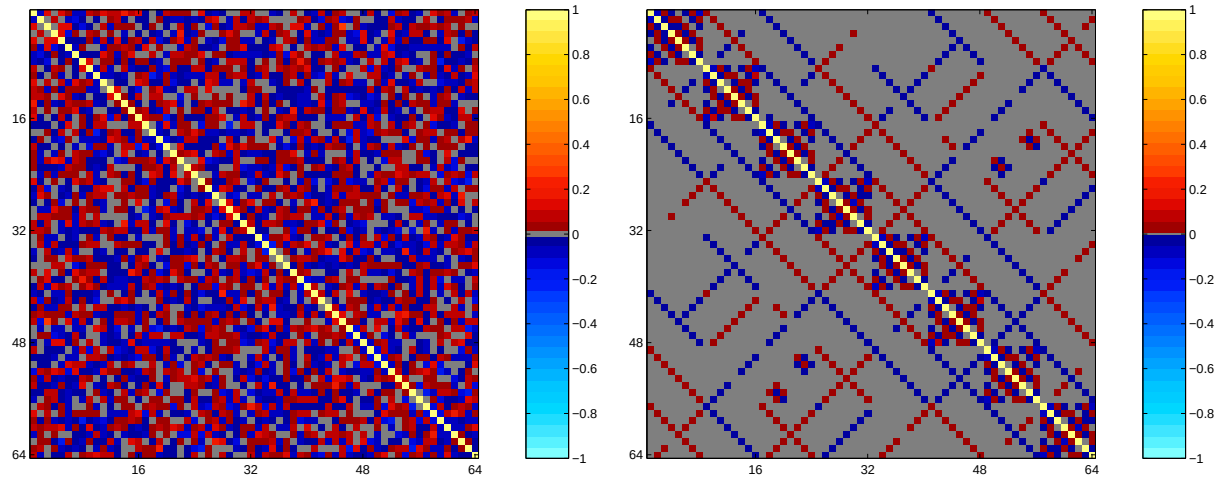

(a) sample between voxels

(b) theoretical between voxels

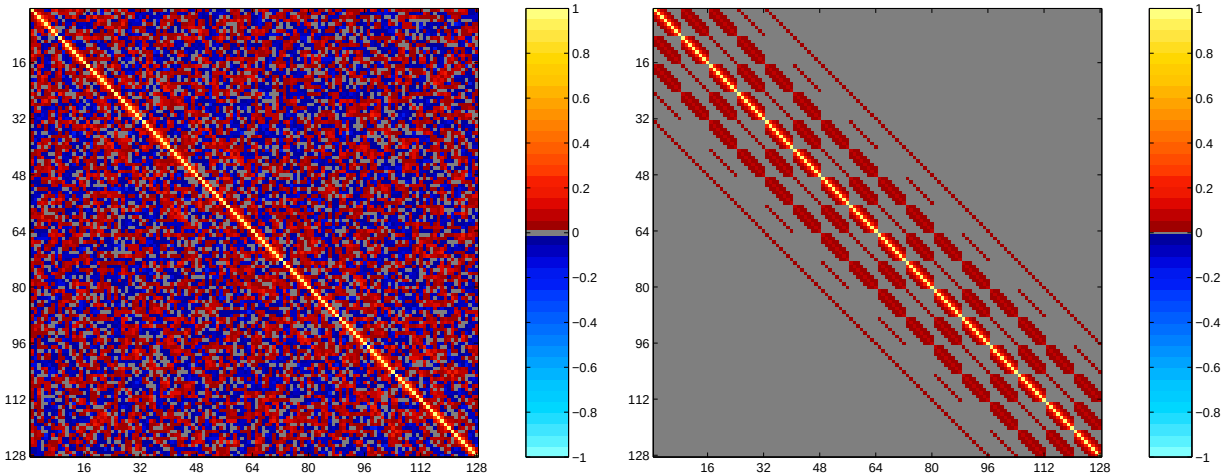

(c) sample between frequencies

(d) theoretical between frequencies

Figure 11: Correlation matrices

permutation matrix P that form the n imaginary measurements within the first second have a 1 in column $t = p + 2, 3p + 2, 5p + 2, ..., 2(n-1)p + p + 2$. This general pattern continues so that the t^{th} row within the $(2p-1)^{th}$ set of n rows of the permutation matrix P that form the n real measurements within the p^{th} voxel have a 1 in column $t = 0p + p, 2p + p, 4p + p, ..., 2(n-1)p + p$. The t^{th} row within the second set of n rows of the permutation matrix P that form the n imaginary measurements within the first second have a 1 in column $t = p + p, 3p + p, 5p + p, ..., 2(n-1)p + p + p$. In general, the j^{th} set of $2n$ rows for the j^{th} voxel, $j = 1, ..., p$ have a 1 in columns $0p + j, 2p + j, 4p + j, ..., 2(n-1)p + j$ of its first n rows for the real voxel measurements and in columns $p + j, 3p + j, 5p + j, ..., 2(n-1)p + p + j$ for the imaginary voxel measurements.

References

[1] P.M. Bandettini, A. Jesmanowicz, E.C. Wong, and J.S. Hyde. Processing strategies for time-course data sets in functional MRI of the human brain. *Magn. Reson. Med.*, 30(2):161–173, 1993.

[2] K.J. Friston, P. Jezzard, and R. Turner. Analysis of functional MRI time-series. *Human Brain Mapp.*, 1(8):153–171, 1994.

[3] E.M. Haacke, R. Brown, M. Thompson, and R. Venkatesan. *Magnetic Resonance Imaging: Principles and Sequence Design*. John Wiley and Sons, New York, 1999.

[4] D.A. Harville. *Matrix Algebra From a Statistician's Perspective*. Springer-Verlag, New York, 1999.

[5] A. Kumar, D. Welti, and R.R. Ernst. NMR Fourier zeugmatography. *J. Magn. Reson.*, 18:69–83, 1975.

[6] B.R. Logan and D.B. Rowe. An evaluation of thresholding techniques in fMRI analysis. *NeuroImage*, 22(1):95–108, 2004.

[7] F.Y. Nan and R.D. Nowak. Generalized likelihood ratio detection for fMRI using complex data. *IEEE Trans. Med. Imag.*, 18(4):320–329, 1999.

[8] D.B. Rowe. Modeling both the magnitude and phase of complex-valued fMRI data. *NeuroImage*, 25(4):1310–1324, 2005a.

[9] D.B. Rowe. Parameter estimation in the magnitude-only and complex-valued fMRI data models. *NeuroImage*, 25(4):1124–1132, 2005b.

[10] D.B. Rowe and B.R. Logan. A complex way to compute fMRI activation. *NeuroImage*, 23(3):1078–1092, 2004.

[11] D.B. Rowe and B.R. Logan. Complex fMRI analysis with unrestricted phase is equivalent to a magnitude-only model. *NeuroImage*, 24(2):603–606, 2005.